Hindawi
Advances in Materials Science and Engineering
Volume 2019, Article ID 5746315, 9 pages
https://doi.org/10.1155/2019/5746315

Research Article

Strength and Deformation Properties of Fiber and Cement Reinforced Heavy Metal-Contaminated Synthetic Soils

Qiang Tang,[1,2] **Peixin Shi**,[1] **Yu Zhang**,[1] **Wei Liu**,[1] **and Lei Chen**[1]

[1]*School of Rail Transportation, Soochow University, Suzhou, China*
[2]*National Engineering Laboratory of Highway Maintenance Technology, Changsha University of Science & Technology, Changsha, China*

Correspondence should be addressed to Peixin Shi; pxshi@suda.edu.cn

Received 29 June 2018; Revised 21 January 2019; Accepted 5 February 2019; Published 19 February 2019

Academic Editor: Ana María Díez-Pascual

Heavy metals are not only hazardous to environment and public health, but they degrade the physicochemical and biological properties of soils increasing difficulty to the redevelopment of contaminated sites. This study proposes a method for reinforcing contaminated soils with fiber and cement. The feasibility of using wheat straw as fiber reinforcement is discussed. The strength of heavy metal-contaminated soil reinforced with wheat straw and cement is investigated through laboratory testing. Twelve groups of soil samples were prepared at three fiber contents (i.e., 0.1%, 0.2%, and 0.3% by weight), three water contents (i.e., 9%, 12%, and 15%), and three cement contents (i.e., 5%, 7.5%, and 10% by weight). Unconfined compression strength (UCS) was tested after 28 days of curing period and various freeze-thaw cycles. The testing results show that the increase in the number of freeze-thaw cycles results in the decrease of UCS. The inclusion of fiber reinforcement within cemented soil causes an increase in the UCS and changes the brittle behavior of cemented soil to a more ductile one. The UCS of the fiber-reinforced soils first increases, then decreases with the increase of water content, and reaches the maximum value at the optimum moisture content.

1. Introduction

With rapid industrialization, soil contamination by heavy metals has become one of the main global environmental problems [1–5]. Heavy metals in soil are highly toxic, persistent, and nonbiodegradable, which will impair the natural ecosystem services and eventually damage human health via the food chain [6–10]. Furthermore, heavy metals have adverse effects on the mechanical properties of soils, which results in unfavorable conditions for the redevelopment of contaminated sites [11]. Solidification/stabilization (S/S) is an effective and economical method to heavy metal-contaminated soil treatment and has attracted increasing attention in the past decades [12, 13]. S/S technology according to different disposal locations can be divided into in situ and ex situ. Ordinary Portland cement, as a common binder utilized in S/S remediation, encapsulates heavy metal ions in a monolithic solid of high structural integrity to reduce further mobility of heavy metal ions [11, 12]. Du et al. evaluated the environmental characteristics of cement-solidified heavy metal-contaminated soil by using the finite element model. The results found that heavy metals leaching concentration is less than the maximum allowable value after the cement-solidified soil as foundation material served 50 years [14]. More importantly, cement-solidified soils have a certain strength and can be used as the bearing material for shallow foundations and base for roadway or railway embankments [11].

Previous studies show that the presence of heavy metals in soils creates a retardant effect on the hydration reaction of cement-based binders [15]. Because the quantity of hydration products (e.g., calcium-silicate-hydrate (C-S-H) gels) in cement-solidified soils is positively correlated with the strength, the retarded formation of hydration products caused by heavy metals leads to a lower strength and modulus [16]. Buj et al. found that the presence of high concentrations of heavy metals noticeably impacted the strength of cemented soil matrix by creating defects at

crystalline matrices [17]. Based on the measured unconfined compressive strength (UCS) of soil samples at different heavy metal concentrations, Du et al. found that the UCS of stabilized Zn-contaminated soils decreased slightly as Zn concentration increased [18]. When exposed to certain long-term external conditions such as freeze-thaw cycling, cracks occur easily in the cement-solidified mixture and the UCS decreases with alternative cycles [19]. Previous studies showed that the initial cracking and subsequent frost lens formation increased the potential to damage of the soil-cement materials [20]. Lake et al. showed that the specimens exposed to freeze-and-thaw conditions were more prone to cracking because the freezing generates excess pressure exceeding the tensile strength of the material [21].

Fiber reinforcement increases the modulus and inhibits cracking of soils. It serves as an effective method to treat cement-solidified heavy metal-contaminated soils. Wheat straw, the residue after wheat harvest, is produced in large quantities worldwide [22]. As a large agricultural country, the annual output of straw in China is about 7 million tons, accounting for about 20~30% of the total amount in the world [23]. Currently, the direct open burning is a major way to destroy the straw in China. The particulate matter and gaseous pollutants released during straw burning create a serious negative effect on the atmospheric environment, climate change, and ecological system [24, 25]. In China, straw open burning may lead to closing of highways and flight delay [26]. The application of agricultural crop residues may open new markets for wheat straw and improve the rural agricultural economy [27]. In this paper, wheat straw and cement were chosen as reinforcing element and solidified material, respectively. Cement seals wheat fibers in a dense matrix to increase strength and durability, and wheat fibers change the brittleness of the cemented soil to a more ductile one. The influence of cement content, water content, quantity of fibers, and alternative cycles of freeze-thaw is evaluated in terms of the compressive strength and failure strain.

2. Materials and Methods

2.1. Materials. To avoid the adverse effects of material in homogeneity on the strength and deformation properties of natural soils, laboratory-made sand-clay mixtures were used for testing. The synthetic soil consisted of 70% sand and 30% kaolin and can be classified as sandy loam texture according to the *Classification and Codes for Chinese Soil* (GB/T 17296-2000). A maximum dry density of 1.88 g/cm^3 and a optimum water content of 12% were determined by the compaction tests based on *Standard for Soil Test Method* (GB/T 50123-1999). Clay is commercial kaolin which was sampled from Suzhou Kaolin Co. Ltd., China. Commercial sand with a mean diameter of approximately 1.0 mm was collected from Shengfa Building Materials Co. Ltd., China. As a solidified material, the commercially available Portland cement (i.e., PG325) was purchased from the cement plant in Anhui, China. The cement mainly consists of 6 ~ 15% active additive and 85~94% cement. The physical properties and chemical composition of the soil and cement are summarized in Table 1. Prior to use, the soil and cement were dried in an oven at a temperature of 105°C for at least 24 hours (101-A, Leao, China) and sieved (1 mm for soils; 0.3 mm for cement) to remove impurities. The chemical, lead nitrate, $Pb(NO_3)_2$ (analytical reagent), was obtained from Suzhou Experiment Instrument Co. Ltd., China. The water used was deionized water (DIW), prepared from tap water via distillation (RFD240NA, Advantec, Japan).

Local wheat straw fibers were used as the reinforcement material. Agroresidues were obtained from local farms and homogenized carefully. The wheat straw is composed (on a mass basis) of 57 ± 10% internodes, 18 ± 3% leaves, 10 ± 2% nodes, 9 ± 4% chaff, and 6 ± 2% rachis [28]. The stem of wheat straw was selected, cleaned, and grouped for pretreatment. The pretreatment process of wheat straw is shown in Figure 1. The wheat straw fibers were dried at the temperature of 65°C [29]. After drying, they were cleaned and the leaves, spikes, sheaths, and fragments were removed. The samples were then collected for microstructure observations using a scanning electron microscope (SEM) (S-4700, Hitachi, Japan). A homogenous group of wheat fibers with approximately equal diameter was selected and chopped into the required length using a grain straw shredder (YB-1000A, Sufeng Industrial, China), operating at 25,000 rpm and equipped with a 200 mm replaceable blade. The wheat straw fibers were kept in sealing bags for storage at room temperature. The straw fibers after milling were about 10~20 mm in length and 2~3 mm in diameter. The fiber compositions of the wheat straw fibers are celluloses, lignin, and hemicelluloses, and the total inorganic content is about 15% [29].

2.2. Experimental Program. As Pb was commonly encountered in contaminated sites worldwide, especially in China, it was selected as the target heavy metal in this work [30]. To reach the target concentration of Pb(II) (1 mg/g and 10 mg/g), a certain dose of $Pb(NO_3)_2$ was dissolved in a small amount of DIW and was then poured into the dry synthetic soil. Unreinforced samples and wheat straw fiber-reinforced samples were homogenized with the cement at three different cement/soil ratios (5%, 7.5%, and 10%) after blending for 2~3 min in a blender. Simultaneously, the exact amount of DIW was weighted and slowly poured into the mixture to prevent fiber segregation during sample formation. The water content of the three specimens was 9%, 12%, and 15%, respectively. Wheat straw fibers were applied as a reinforcement material at the percentage of 0.1, 0.2, and 0.3 by weight of soil. The mixing process for the soil, water, cement, and fibers was stopped when the fibers were evenly distributed and randomly oriented throughout the soil. After mixing, the mixture was shaped in a mold with a length of 100 mm and an inner diameter of 50 mm with full compaction. To ensure uniformity, the samples were compacted in five layers. The height of each layer was approximately 1/5 of the specimen height. A rammer was dropped 12 times from a height of 200 mm on each layer of the specimen. After that, the mixtures were demolded and cured (90 ± 2% humidity; 20 ± 2°C) for 28 days in a curing box (HBY-15B,

Table 1: Properties of soils and cement.

Property	Standard	Unit	Kaolin	Sand	Cement
Moisture	JIS A 1203	%	2.90	0.39	0.5
pH	JGS 0211		4.70	7.50	10
EC	JGS 0212	mS/cm	0.42	0.06	
Grain size distribution	GB/T 50123-1999				
Clay fraction (≤0.005 mm)		%	56.40	0.10	2.3
Silt fraction (0.075–0.005 mm)		%	18.80	2.98	97.7
Sand fraction (2-0.075 mm)		%	24.80	96.92	0
N_2-BET					
Correlation coefficient (R^2)			0.99	0.99	0.99
Specific surface area		m^2/g	29.41	0.014	0.35
Diameter		nm	29.97		
Pore volume		cm^3/g	0.22		
Chemical composition					
SiO_2		%	45.32	93.57	1.94
Fe_2O_3		%	0.14	0.74	0.23
CaO		%	0.02	1.87	31.31
Al_2O_3		%	51.13	2.12	0.9
MgO		%	0.28	0.28	0.29
SO_3		%	0.09		43.49
TiO_2		%	0.68	0.027	
Na_2O		%	0.56	0.48	
K_2O		%	1.54	0.59	
Cl^-		%	0.01		

(a) (b) (c) (d)

Figure 1: Pretreatment process of wheat straw. (a) Local wheat straw fibers. (b) Cleaned and dried fibers. (c) Milled fibers. (d) Fibers kept in a sealing bag.

Donghua, China). Table 2 provides the details of the different water, cement, and fiber content of the mixtures. Three replicates were analyzed for each set of testing.

During freezing and thawing, the specimens were placed into a refrigerator at −10°C for 6 hrs and then at +10°C for thawing phase for 6 hrs as suggested by Qi et al. [31]. Observation during testing shows that, after the six-hour freezing or thawing, the specimen height keep virtually remains constant. The unreinforced samples were subjected to 0, 3, 6, and 9 freeze-thaw cycles, and the wheat straw fiber-reinforced samples were subjected to 9 freeze-thaw cycles. The UCS of the unreinforced and wheat straw fiber-reinforced soil samples was tested as per ASTM D 2166-91 using a microcomputer-controlled electronic testing machine (LDS-50, Chenda, China) with a strain rate of 1 mm/min. The testing machine (MTS 10/GL) has a loading capacity of 50 kN, as referenced to the study of Koohestani et al. [32]. The loads were recorded at the point of sample fracturing, and the UCS was determined using the formula $P = F/A$, where P is the compressive strength (MPa), F is the load (N) at fracture, and A is the area of loading cross section (mm^2). All the tests were replicated, and the average values were reported.

3. Results and Discussion

3.1. Results. It is well documented that the USC and failure strain of cement-based samples can reflect directly the degree of deterioration caused by freeze-thaw attacks. Figure 2 shows the variation of the UCS of the cement-based solidification samples under different freeze-thaw cycles. Figure 3 shows the variation of the failure strain of the samples subjected to different freeze-thaw cycles. As seen in Figure 2, the maximum UCS is achieved with the specimens free from freeze-thaw cycles. The UCS decreased with alternative cycles. Figure 2(a) shows that the largest strength reduction was about 56.1% that occurred after the 9th cycle.

Table 2: Composition and properties of the soil mixtures.

Cycles	Pb concentration (%)	Water content (%)	Cement content (%)	Fiber content (%)
Unreinforced				
0	0.1	9	7.5	0
		12	7.5	0
		15	7.5	0
	1	12	5	0
		12	7.5	0
		12	10	0
3	0.1	9	7.5	0
		12	7.5	0
		15	7.5	0
	1	12	5	0
		12	7.5	0
		12	10	0
6	0.1	9	7.5	0
		12	7.5	0
		15	7.5	0
	1	12	5	0
		12	7.5	0
		12	10	0
9	0.1	9	7.5	0
		12	7.5	0
		15	7.5	0
	1	12	5	0
		12	7.5	0
		12	10	0
Reinforced				
9	0.1	9	7.5	0.1
		9	7.5	0.2
		9	7.5	0.3
		12	7.5	0.1
		12	7.5	0.2
		12	7.5	0.3
		15	7.5	0.1
		15	7.5	0.2
		15	7.5	0.3
	1	12	5	0.1
		12	5	0.2
		12	5	0.3
		12	7.5	0.1
		12	7.5	0.2
		12	7.5	0.3
		12	10	0.1
		12	10	0.2
		12	10	0.3

According to Mehta and Monteiro, the pores in hardened cement paste can be divided into three main groups according to their form and size: capillary, gel, and air pores [33]. During the freezing and thawing processes, water firstly enters the biggest pores of hardened cement paste and subsequently reaches the smaller pores. According to Everett, ice crystals in the pores tend to grow continuously and penetrate deeper into smaller pores of the hardened cement paste and thus fill capillary pores with water or freezing solution [34]. When water or freezing solution freezes, the volume of water stored in micropores increases by 9%, the hardened cement paste generates internal stresses, and finally crumbles [35, 36].

Cement treatment strengthens the fabric of clays at the intercluster spacing and forms strong bonds with the fabric. According to Kalliopi, the destructive effect during freezing depends on the content of water in hardened cement paste [37]. Figure 2(a) shows that the UCS of the samples increased when the water content increased from 9% to 12% but decreased when the water content increased from 12% to 15%, indicating that there is a threshold value of water content beyond which the UCS decreases with increasing water content. This is because that, with high water content, the cohesive force of the soil subject to freeze-thaw cycles is lower than that before freeze-thaw cycles. The growth of ice crystals destroys the connection between soil particles and the structure of products of hydration.

The effects of freeze-thaw cycles on the UCS varied depending on the cement percentage added to the specimens. Figure 2(b) shows that the UCS increased with the increase of cement content after 9 freeze-thaw cycles. The UCS of the unreinforced samples with 5%, 7.5%, and 10% cement were 0.06, 0.26 and 0.44 MPa, respectively. The increase in strength reflected the ongoing hydration reaction during which the strong adhesive products (e.g., C-H-S gels) were generated to provide high bearing capacity against loading [38]. Figure 3(b) shows the ductility of the samples decreased with the increase of cement content. After 9 freeze-thaw cycles, the failure strain of the mixtures with 5%, 7.5%, and 10% cement was 0.7%, 0.63%, and 0.57%, respectively.

Figure 2 further shows that the concentration of heavy metal had a significant impact on the strength of cement stabilized soil. For the 12% water + 7.5% cement samples, the increase of the Pb(II) concentration from 1 mg/g (0.1%, Figure 2(a)) to 10 mg/g (1%, Figure 2(b)) resulted in a decrease of the UCS by 71.9%, 83.3%, 87.4%, and 86.2%, respectively, after subjecting to 0, 3, 6, and 9 freeze-thaw cycles, respectively. This is because the presence of Pb(II) has a negative effect on the hydration reaction of cement and hinders the hydration reaction of cement.

Figures 4 and 5 plot the UCS and the failure strain of wheat straw-reinforced samples with various fiber percentages subjecting to 9 freeze-thaw cycles, respectively. These figures show that the addition of wheat straw increased the UCS of soil and restrained the deformation of the samples. As shown in Figure 4(b), the maximum values of UCS observed in 0.1% fiber with 5%, 7.5%, and 10% cement content were 1.47, 1.59, and 2.9 MPa, respectively, which were 24.5, 6.1, and 6.6 times higher than that of unreinforced samples.

Figure 4(a) shows that, with the increase of the fiber content, the UCS increased first, reached the maximum value when the fiber content was 0.1%, and then reduced. Figure 4(a) also shows that, with the increase of the water content, the UCS increased when the water content was relatively low (e.g., 9% and 12%). When the water content was relatively high (e.g., 15%), the UCS kept virtually constant or decreased, depending on the fiber content. Taking 0.2% fiber as an example, the UCS of the reinforced soil with 9, 12, and 15% water content was 3.25, 5.18, and 3.45 MPa, respectively.

The failure strains obtained from the unconfined compression tests are given in Figure 5. The comparison with the

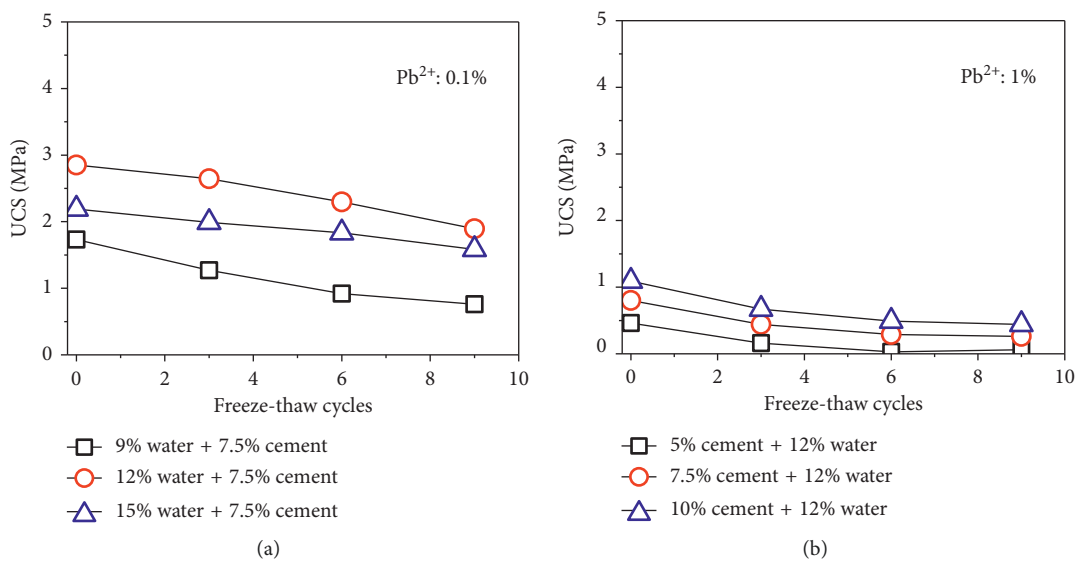

Figure 2: UCS of unreinforced samples during freeze-thaw cycles. (a) Various percentages of water content based on 7.5% cement + 0.1% Pb(II). (b) Various percentages of cement content based on 12% water + 1% Pb(II).

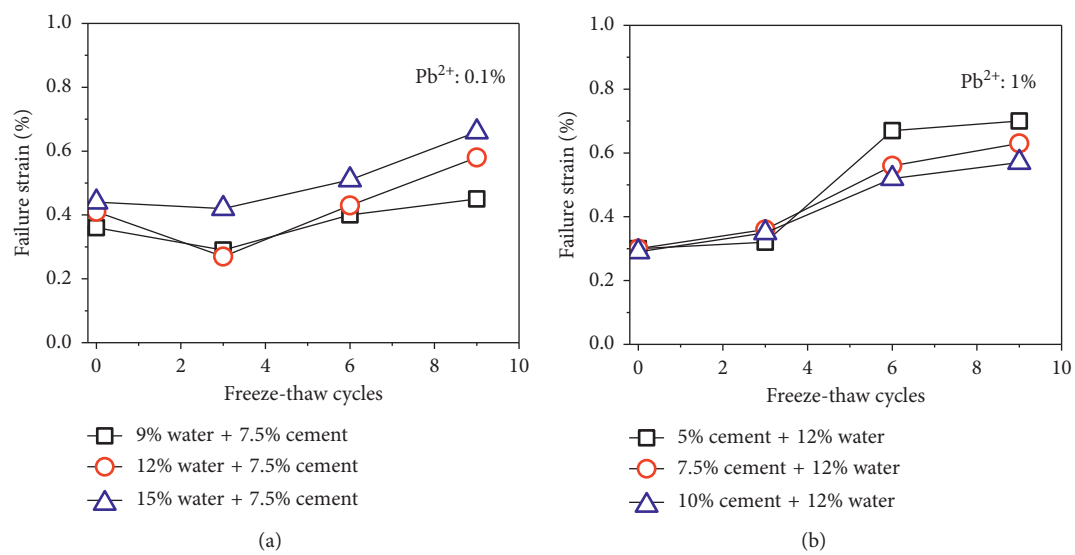

Figure 3: Failure strain of unreinforced soil samples during freeze-thaw cycles. (a) Various percentages of water content based on 7.5% cement + 0.1% Pb(II). (b) Various percentages of cement content based on 12% water + 1% Pb(II).

unreinforced samples shows that the inclusion of fibers within the cemented soil reduced the failure strain. As shown in Figure 5(a), the failure strain of three different cement content samples with 0.1% fiber is 0.33 (5% cement), 0.31 (7.5% cement), and 0.43% (10% cement), respectively. Compared with unreinforced samples, the failure strains of cement-fiber samples reduce by 52.9%, 50.8%, and 24.6%. As such, the fibers incorporated into cement-based material increase the deformation resistance of the samples by inhibiting the crack generation with the samples.

3.2. Mechanism. The test results in this study suggest that the strength and deformation behaviors of cemented soil reinforced by wheat straw were considerably affected by fiber content, cement content, and water content. The integrality and strength of reinforced soil can be enhanced by inclusion of randomly distributed wheat straw, and the deformation can be restrained. It is generally agreed that reinforcement plays an important role in the development of UCS. The distributed discrete fibers act as a spatial three-dimensional network to interlock soil grains, help grains to form a unitary coherent matrix, and restrict the displacement. Consequently, the stretching resistance between clay particles and strength was improved. As a natural fiber material, wheat straw has tensile strength which makes it suitable for soil reinforcement [39]. Because of the interfacial force, the fibers in the matrix are difficult to slide and can acquire tensile stress, as the schematic diagram shown in Figure 6. When the specimens are under tension, the "bridge" effect of the

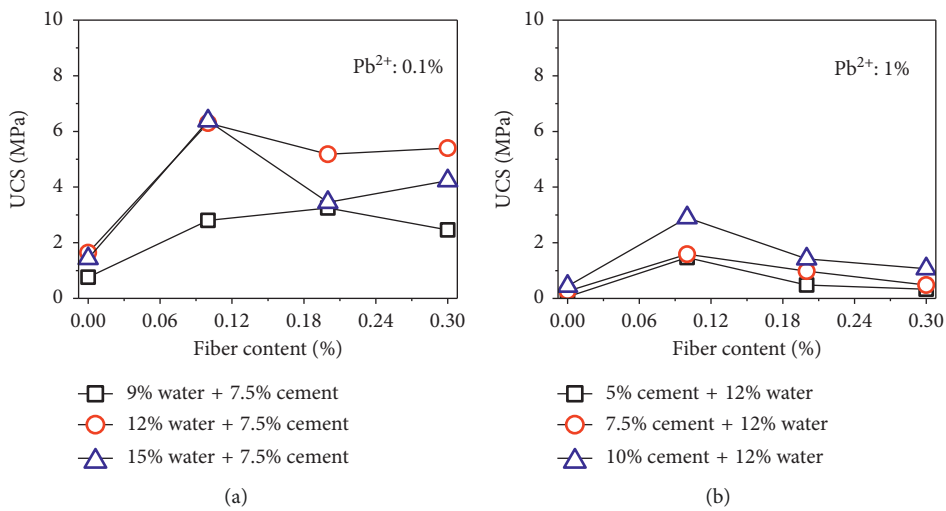

Figure 4: UCS of fiber-reinforced samples under 9 cycles. (a) Various percentages of water content based on 7.5% cement + 0.1% Pb(II). (b) Various percentages of cement content based on 12% water + 1% Pb(II).

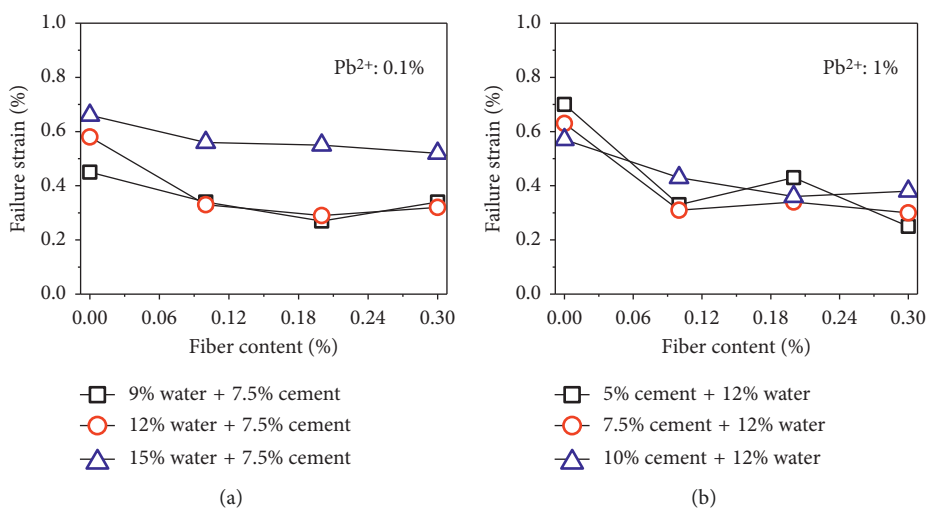

Figure 5: Failure strain of fiber-reinforced soil samples under 9 cycles. (a) Various percentages of water content based on 7.5% cement + 0.1% Pb(II). (b) Various percentages of cement content based on 12% water + 1% Pb(II).

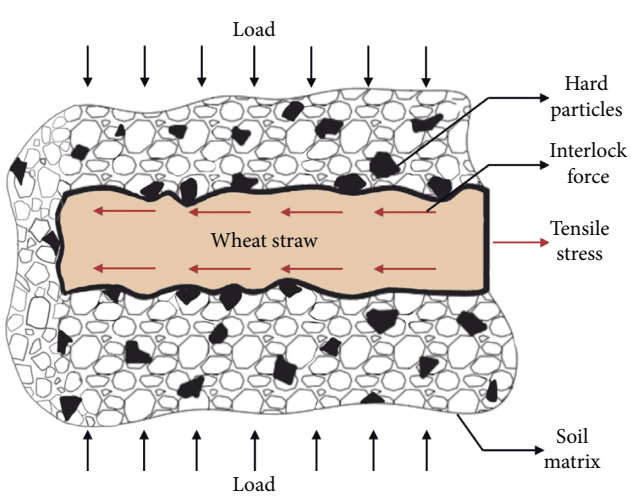

Figure 6: Schematic diagram of interfacial interaction between wheat straw and soil.

fibers, as shown in Figure 7, can efficiently impede further development of tensile cracks and deformation of the soil. As a result, the fiber-reinforced soil demonstrated a more ductile behavior.

Several studies indicated that the fiber sliding resistance was strongly dependent on the fiber surface roughness [40–42]. As the fibers were mixed and the samples were compacted, the hard particles (such as sands) of mixtures impacted and abraded the fiber surface, causing plastic deformation and even removal of part of the surface layer. The pits and grooves formed on the fiber surface constituted an interlock and improved the interactions between fiber surface and soil matrix. The SEM observations on the surface of wheat straw, as presented in Figure 8, show that the wheat straw surface was covered by pits and grooves. The addition of wheat straw fiber leads to a significant increase in UCS of the soil samples, and there is an optimum wheat fiber content at which the UCS reaches maximum according to

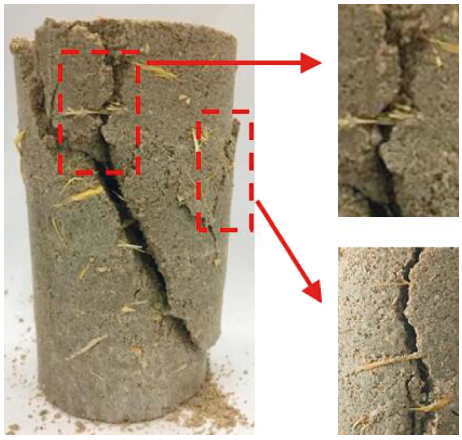

Figure 7: "Bridge" effect of wheat straw in cemented soil.

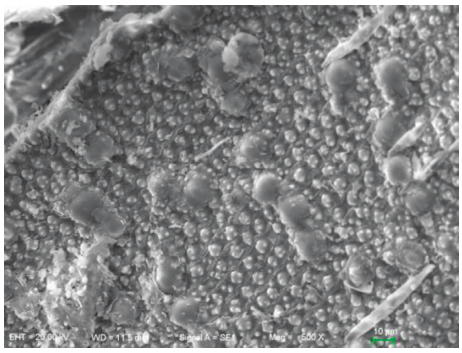

Figure 8: SEM images of wheat straw.

the study Qu and Sun; if the fiber content exceeds the optimum content, fiber overlapping may occur [43]. The frictional resistance between fibers is smaller than that between soil particle and fiber. In this case, increasing fiber content will lower the strength of reinforced soil. Prabhakara and Sridhar also come to the similar conclusion. This is the reason for the reduction of UCS after 0.1% fiber content [44].

It should be noted that wheat straw fibers are very easily affected by the presence of salts in soils, biological degradation, and ultraviolet degradation. Only when the wheat straw fibers are wrapped up to block its direct contact with water and air, they may be spared from the environmental degradation [45]. According to Tang et al., the fiber surface is attached by hydrated products of the cement [46]. It is known that the by-products of the cement possess higher strength and cementation than that of the clay grains. Therefore, the strength of fiber-reinforced cemented soil increases with increasing cement content. Network-like hydration crystals were wrapped around the fiber tightly that effectively restricted the fiber's relative movement and increased the reinforcement benefit significantly. The high degree of stiffness of the attached hydration crystals also toughened the distributed fibers, which act similarly to plant roots in distributing the stresses in a broader area and inhibiting fissure propagation. Therefore, the combined fiber and cement inclusions increase the efficiency of transfer of the load from matrix to fibers. Furthermore, the hydration of the cement binds soil particles together and makes the matrix more compacted, causing an increase in normal stress around the fiber body and the effective contact area. Tagnit-Hamou et al. considered that, during cement hydration, the exothermic effect causes localized damage to the surface of the fibers [41]. The hardness of the superficial layer decreases and allows the insertion of crystals. Meanwhile, during mixing, filler grains cause grooves and stripping. Fiber roughness increases and allows a better adherence to the paste which results in the static friction coefficient between fiber and composite matrix increased [41, 46].

With the increase of water content, the UCS of fiber-reinforced samples first increases and then decreases. This phenomenon indicates that the moisture content has a significant impact on the UCS of wheat straw-reinforced soil. Only when the water content of reinforced soil reaches a certain value can wheat straw produce the best result. The low water content will lead to the drying of the soil, and the deformation of the reinforcement and the soil cannot be coordinated. According to Huang et al., the cohesive function between hydrated film and soil particles will gradually increase with the increase of water content when the water content is less than the optimum moisture content [47, 48]. The increase of cohesive force improves the friction between wheat straw and soil so that the tensile properties of straw are fully reflected, resulting in an increase of the UCS. However, with the increase of water content, the hydrated film around soil grains thickens, improving the lubrication between the reinforcement and soil grains. Furthermore, when the hydrated film in the contact of soil particles is squeezed, the bounded water becomes free water and reduces the cohesive force of soil.

4. Conclusions

In this paper, a series of experiments were conducted to evaluate the effects of randomly distributed short wheat straw fiber reinforcement on the strength behavior of cemented soils. The effect of wheat straw fiber and cement inclusions on UCS, failure strain, and elastic modulus of heavy metal-contaminated soil specimens was determined. According to the testing results, the mechanical properties of reinforced soil change with increasing the fiber content until an optimum content at which the UCS of the reinforced soil reaches maximum. The optimum fiber content is found to be 0.1% in the current tests.

The addition of fibers can effectively prevent the damage caused by freeze-thaw cycles to the soils. The "bridge" effect of wheat straw can efficiently impede the further development of tensile cracks and deformation of the soil. Increasing cement content could increase the UCS and decrease the failure strains of fiber-reinforced cemented soil. The by-products of the cement possess higher strength and cementation than those of the clay grains. In fiber-reinforced cemented soil, the interactions between the fiber surface and the hydrated products play a major role on the strength characteristic. On account of above findings, it is recommended that, in cold climates, where soil is affected by freeze-thaw cycles, wheat fibers can be applied in the field of geotechnical engineering from an environmental point of view.

Data Availability

All the data presented in the manuscript were obtained from laboratory tests at Soochow University in Suzhou, China. All the laboratory testing data were presented in the figures and tables in the manuscript. We will be very pleased to share our all the raw data. If needed, please contact the corresponding author.

Conflicts of Interest

The authors declare that they have no conflicts of interest.

Acknowledgments

This research was funded by the National Nature Science Foundation of China (51778386 and 51708377), Open Fund of National Engineering Laboratory of Highway Maintenance Technology (Changsha University of Science & Technology) (kfj180105), Natural Science Foundation of Jiangsu Province (BK20170339), and Project from Jiangsu Provincial Department of Housing, Urban-Rural Development (2016ZD18 and 2017ZD002).

References

[1] Q. Tang, F. Gu, Y. F. Gao, T. Inui, and T. Katsumi, "Desorption characteristics of Cr(III), Mn(II) and Ni(II) in contaminated soil using citric acid and citric acid containing wastewater," *Soils and Foundations*, vol. 58, no. 1, pp. 50–64, 2018.

[2] Q. Tang, H. J. Kim, K. Endo, T. Katsumi, and T. Inui, "Size effect on lysimeter test evaluating the properties of construction and demolition waste leachate," *Soils and Foundations*, vol. 55, no. 4, pp. 720–736, 2015.

[3] Y. Zhang, Q. Tang, S. Chen, F. Gu, and Z. Z. Li, "Heavy metal adsorption of a novel membrane material derived from senescent leaves: kinetics, equilibrium and thermodynamic studies," *Membrane Water Treat*, vol. 9, no. 2, pp. 95–104, 2018.

[4] Q. Tang, F. Gu, Y. Zhang, Y. Zhang, and J. Mo, "Impact of biological clogging on the barrier performance of landfill liners," *Journal of Environmental Management*, vol. 222, pp. 44–53, 2018.

[5] Q. Tang, T. Katsumi, T. Inui, and Z. Li, "Influence of pH on the membrane behavior of bentonite amended Fukakusa clay," *Separation and Purification Technology*, vol. 141, pp. 132–142, 2015.

[6] Q. Tang, T. Katsumi, T. Inui, and Z. Li, "Membrane behavior of bentonite-amended compacted clay," *Soils and Foundations*, vol. 54, no. 3, pp. 329–344, 2014.

[7] Q. Tang, X. Tang, Z. Li et al., "Zn(II) removal with activated firmiana simplex leaf: kinetics and equilibrium studies," *Journal of Environmental Engineering*, vol. 138, no. 2, pp. 190–199, 2012.

[8] Q. Tang, X. Tang, M. Hu, Z. Li, Y. Chen, and P. Lou, "Removal of Cd(II) from aqueous solution with activated Firmiana Simplex Leaf: behaviors and affecting factors," *Journal of Hazardous Materials*, vol. 179, no. 1–3, pp. 95–103, 2010.

[9] Q. Tang, T. Zhou, F. Gu, Y. Wang, and J.-m. Chu, "Removal of Cd(II) and Pb(II) from soil through desorption using citric acid: kinetic and equilibrium studies," *Journal of Central South University*, vol. 24, no. 9, pp. 1941–1952, 2017.

[10] Q. Tang, W. Liu, Z. Li, Y. Wang, and X. Tang, "Removal of aqueous Cu(II) with natural kaolin: kinetics and equilibrium studies," *Environmental Engineering and Management Journal*, vol. 17, no. 2, pp. 467–476, 2018.

[11] Q. Tang, Y. Zhang, Y. Gao, and F. Gu, "Use of cement-chelated, solidified, municipal solid waste incinerator (MSWI) fly ash for pavement material: mechanical and environmental evaluations," *Canadian Geotechnical Journal*, vol. 54, no. 11, pp. 1553–1566, 2017.

[12] Q. Tang, Y. Liu, F. Gu, and T. Zhou, "Solidification/stabilization of fly ash from a municipal solid waste incineration facility using Portland cement," *Advances in Materials Science and Engineering*, vol. 2016, Article ID 7101243, 10 pages, 2016, in press.

[13] J. H. Zhang, J. H. Peng, J. L. Zheng, L. J. Dai, and Y. S. Yao, "Prediction of resilient modulus of compacted cohesive soil in south China," *International Journal of Geomechanics*, vol. 10, no. 6, pp. 248-249, 2019.

[14] P. X. Du, Y. Zhang, W. Y. Wei, and Q. Tang, "Strength and environmental characteristics of cement solidified heavy metal contaminated soil: experiment and numerical simulation," *Science, Engineering, and Technology*, vol. 18, no. 21, pp. 146–154, 2018.

[15] X. Li, C. S. Poon, and H. Sun, "Heavy metal speciation and leaching behaviors in cement based solidified/stabilized waste materials," *Journal of Hazardous Materials*, vol. 82, no. 3, pp. 215–230, 2001.

[16] S. H. Chew, A. H. M. Kamruzzaman, and F. H. Lee, "Physicochemical and engineering behavior of cement treated clays," *Journal of Geotechnical and Geoenvironmental Engineering*, vol. 130, no. 7, pp. 696–706, 2004.

[17] I. Buj, J. Torras, D. Casellas, M. Rovira, and J. de Pablo, "Effect of heavy metals and water content on the strength of magnesium phosphate cements," *Journal of Hazardous Materials*, vol. 170, no. 1, pp. 345–350, 2009.

[18] Y.-J. Du, M.-L. Wei, K. R. Reddy, F. Jin, H.-L. Wu, and Z.-B. Liu, "New phosphate-based binder for stabilization of soils contaminated with heavy metals: leaching, strength and microstructure characterization," *Journal of Environmental Management*, vol. 146, pp. 179–188, 2014.

[19] Z. He, S. W. Tang, G. S. Zhao, and E. Chen, "Comparison of three and one dimensional attacks of freeze-thaw and carbonation for concrete samples," *Construction and Building Materials*, vol. 127, pp. 596–606, 2016.

[20] M. A. Othman and C. H. Benson, "Effect of freeze-thaw on the hydraulic conductivity and morphology of compacted clay," *Canadian Geotechnical Journal*, vol. 30, no. 2, pp. 236–246, 1993.

[21] C. B. Lake, A. M. Yousif, and R. J. Jamshidi, "Examining freeze/thaw effects on performance and morphology of a lightly cemented soil," *Cold Regions Science and Technology*, vol. 134, pp. 33–44, 2016.

[22] S. Panthapulakkal and M. Sain, "The use of wheat straw fibres as reinforcements in composites," in *Biofiber Reinforcements in Composite Materials*, O. Faruk and M. Sain, Eds., pp. 423–453, Woodhead Publishing India, Ltd., Delhi, India, 2015.

[23] Y. Bi, C. Y. Gao, Y. J. Wang, and B. Y. Li, "Estimation of the amount of Chinese straw resources," *Chinese Society of Agricultural Engineering*, vol. 25, no. 12, pp. 211–217, 2009.

[24] B. A. M. Radzi, D. R. Oros, and B. R. Simoneit, "Biomass burning as the main source of organic aerosol particulate matter in Malaysia during haze episodes," *Chemosphere*, vol. 55, no. 8, pp. 1089–1095, 2004.

[25] L. Hong, G. Liu, L. Zhou, J. Li, H. Xu, and D. Wu, "Emission of organic carbon, elemental carbon and water-soluble ions from crop straw burning under flaming and smoldering conditions," *Particuology*, vol. 31, no. 2, pp. 181–190, 2017.

[26] Y. Guan, G. Chen, Z. Cheng, B. Yan, and L. a. Hou, "Air pollutant emissions from straw open burning: a case study in tianjin," *Atmospheric Environment*, vol. 171, pp. 155–164, 2017.

[27] S. Panthapulakkal, M. Sain, and M. Sain, "Preparation and characterization of wheat straw fibers for reinforcing application in injection molded thermoplastic composites," *Bioresource Technology*, vol. 97, no. 2, pp. 265–272, 2006.

[28] S. H. Ghaffar and M. Fan, "An aggregated understanding of physicochemical properties and surface functionalities of wheat straw node and internode," *Industrial Crops and Products*, vol. 95, pp. 207–215, 2017.

[29] M. Li, S. Xi Chai, H. Yuan Zhang, H. Pu Du, and L. Wei, "Feasibility of saline soil reinforced with treated wheat straw and lime," *Soils and Foundations*, vol. 52, no. 2, pp. 228–238, 2012.

[30] Y.-J. Du, M.-L. Wei, K. R. Reddy, Z.-P. Liu, and F. Jin, "Effect of acid rain pH on leaching behavior of cement stabilized lead-contaminated soil," *Journal of Hazardous Materials*, vol. 271, no. 4, pp. 131–140, 2014.

[31] J. L. Qi, J. M. Zhang, and Y. L. Zhu, "Influence of freezing–thawing on soil structure and its soils mechanics significance," *Chinese Journal of Rock Mechanics and Engineering*, vol. 22, pp. 2690–2694, 2004.

[32] B. Koohestani, T. Belem, A. Koubaa, and B. Bussière, "Experimental investigation into the compressive strength development of cemented paste backfill containing Nano-silica," *Cement and Concrete Composites*, vol. 72, pp. 180–189, 2016.

[33] P. K. Mehta and P. J. Monteiro, *Concrete Structure, Properties and Materials*, Prentice-Hall, Englewood Cliff, NJ, USA, 2nd edition, 1993.

[34] D. H. Everett, "The thermodynamics of frost damage to porous solids," *Transactions of the Faraday Society*, vol. 57, no. 5, pp. 1541–1551, 1961.

[35] D. H. Everett and J. M. Haynes, "Capillary properties of some model pore systems with special reference to frost damage," *RILEM Bulletin*, vol. 27, pp. 31–36, 1965.

[36] F. Gu, W. Ma, R. C. West, A. J. Taylor, and Y. Zhang, "Structural performance and sustainability assessment of cold central-plant and in-place recycled asphalt pavements: a case study," *Journal of Cleaner Production*, vol. 208, pp. 1513–1523, 2019.

[37] K. A. Kalliopi, "Pore structure of cement-based materials: testing, interpretation and requirements,"*Series: Modern Concrete Technology*, Vol. 12, pp. 1–33, CRC Press, Boca Raton, FL, USA, 2006.

[38] Y.-S. Wang, J.-G. Dai, L. Wang, D. C. W. Tsang, and C. S. Poon, "Influence of lead on stabilization/solidification by ordinary Portland cement and magnesium phosphate cement," *Chemosphere*, vol. 190, pp. 90–96, 2018.

[39] O. Onuaguluchi and N. Banthia, "Plant-based natural fibre reinforced cement composites: a review," *Cement and Concrete Composites*, vol. 68, pp. 96–108, 2016.

[40] S. P. Shah, "Do fibers increase the tensile strength of cement-based matrixes?," *ACI Materials Journal*, vol. 88, no. 6, pp. 595–602, 1991.

[41] A. Tagnit-Hamou, Y. Vanhove, and N. Petrov, "Microstructural analysis of the bond mechanism between polyolefin fibers and cement pastes," *Cement and Concrete Research*, vol. 35, no. 2, pp. 364–370, 2005.

[42] J. D. Frost and J. Han, "Behavior of interfaces between fiber-reinforced polymers and sands," *Journal of Geotechnical and Geoenvironmental Engineering*, vol. 125, no. 8, pp. 633–640, 1999.

[43] J. Qu and Z. Sun, "Strength behavior of shanghai clayey soil reinforced with wheat straw fibers," *Geotechnical and Geological Engineering*, vol. 34, no. 2, pp. 515–527, 2015.

[44] J. Prabhakara and R. S. Sridhar, "Effect of random inclusion of sisal fibre on strength behaviour of soil," *Construction and Building Materials*, vol. 16, no. 2, pp. 123–131, 2002.

[45] L. Wei, S. X. Chai, and H. Z. Cai, "Evaluation of anticorrosive measures for wheat straw and strengthening mechanism of reinforced saline soil in littoral area," *Geotechnical investigation Surveying*, vol. 37, no. 1, pp. 5–7, 2009.

[46] C. Tang, B. Shi, W. Gao, F. Chen, and Y. Cai, "Strength and mechanical behavior of short polypropylene fiber reinforced and cement stabilized clayey soil," *Geotextiles and Geomembranes*, vol. 25, no. 3, pp. 194–202, 2007.

[47] K. Huang, J. W. Wran, G. Chen, and Y. Zeng, "Testing study of relationship between water content and shear strength of unsaturated soils," *Rock and Soil Mechanics*, vol. 33, no. 9, pp. 2600–2604, 2012.

[48] J. Li, J. Zhang, G. Qian, J. Zheng, and Y. Zhang, "Three-dimensional simulation of aggregate and asphalt mixture using parameterized shape and size gradation," *Journal of Materials in Civil Engineering*, vol. 31, no. 3, article 04019004, 2019.